Vapor-phase nucleation of individual CdSe nanostructures from shape-engineered nanocrystal seeds

A. Fasoli, S. Pisana, and A. Colli[a)]
Engineering Department, Cambridge University, Cambridge CB3 0FA, United Kingdom

L. Carbone and L. Manna
National Nanotechnology Laboratory of CNR-INFM, Unità di Ricerca IIT, via per Arnesano km. 5, I-73100 Lecce, Italy

A. C. Ferrari[b)]
Engineering Department, Cambridge University, Cambridge CB3 0FA, United Kingdom

(Received 29 October 2007; accepted 27 November 2007; published online 14 January 2008)

We investigate the vapor-phase nucleation of CdSe nanostructures on nanocrystals seeds of different shapes. The growth dynamics is assessed by transmission electron microscopy, following the evolution of the same nanocrystals prior and after the deposition process. We prove that individual nanocrystals can sustain the growth of single nanowires and determine their final morphology. Straight or branched nanowires are obtained from spherical or tetrapod-shaped nanocrystals, respectively. When tetrapod-shaped nanocrystals are used, we also find that their original shape and orientation are mostly preserved upon further growth. © *2008 American Institute of Physics*. [DOI: 10.1063/1.2825425]

High-aspect-ratio nanostructures made of II-VI compounds have a great potential for applications in optoelectronics.[1–4] Vapor-phase,[5–7] solution-[8–10] or template-assisted[11,12] techniques are routinely employed to controllably synthesize them in a variety of different shapes, such as spheres, rods, ribbons, and multipods.[8,13–16] In vapor-phase synthesis, a metal seed is often used to trigger the growth of one-dimensional (1D) structures selectively on the substrate.[6,15,17] Yet, alternative strategies are investigated to avoid metal contamination. E.g., for polar compounds with a wurtzite structure, metal-free anysotropic growth may occur, since the difference in surface energy along specific crystallographic directions is high enough to drive 1D elongation.[18] However, in this regime, nanowires (NWs) typically nucleate on random locations.[19] To ensure nucleation selectivity into regular patterns it was proposed to use solution-grown nanocrystals as seeds for vapor-phase NW growth.[10,20–22] This approach brings in principle several advantages: (a) shape and size distribution of the seeds can be accurately controlled *a priori*;[8,23] (b) nanocrystal seeds could be deterministically patterned on functionalized substrates;[22,24] and (c) they can be made of the same material of the final NWs, thus, minimizing chemical contaminations.[20]

Although nanocrystal-seeded growth has proven viable for NWs synthesis,[10,20,21,24] many fundamental questions about the nucleation process remain unanswered. First, in contrast to metal-catalyzed growth, the diameter of the final NW is usually much larger than that of the initial seeds.[10,20,21] It is, therefore, unclear if a single NW can arise from a single seed or if a cluster of some critical size is needed to trigger the nucleation process. Second, several groups synthesized shape-controlled nanostructure by varying the growth conditions (temperature, pressure, etc.),[5,6,15,20] but no study has been reported showing, for fixed parameters, the deterministic effect of the seed shape on the final morphology.

Here, we investigate the vapor-phase growth dynamics of CdSe nanostructures, which selectively nucleate on CdSe seeds of different morphology. We focus on CdSe as a test system, since it is one of the most utilized materials for solution-phase synthesis of spherical, rodlike or branched colloidal nanocrystals.[8] We show that, for fixed growth conditions, the synthesis of straight NWs is dominant if spherical nanocrystals (*s*-NCs) are used, whereas branched structures [multipods (MPs)] are obtained from tetrapod-shaped nanocrystals (*t*-NCs). We then assess the early stages of the nucleation process by marking individual precursor seeds on a 50-nm-thick SiN membrane and analyzing by transmission electron microscopy (TEM) the corresponding structure after vapor-phase growth. We show that NWs can stem individually from isolated spherical seeds, and that most branched structures tend to maintain the geometry and orientation of the original tetrapod.

CdSe *s*-NCs (5–10 nm diameter) or *t*-NCs (5–10 nm diameter, 50–100 nm branch length) are produced by a solution phase approach and then dissolved in toluene.[14,23] They are then ultrasonicated for 5 min to reduce aggregation. Subsequently, they are dispersed by spin casting onto Si substrates or onto 50-nm-thick SiN membranes suitable for TEM (Philips Tecnai 20). In the latter case, NCs are individually mapped by TEM via reference markers patterned on the membrane window.[25] All the seed-coated substrates are placed in a single-zone furnace where CdSe nanostructures are grown by thermal evaporation and vapor transport of CdSe powders.[20] Our deposition system allows precise, real-time control of the substrate temperature (T_s), and a pressure-based shutter ensures steady-state growth conditions.[15] A *high growth rate* ($\sim 1\ \mu$m/h) is obtained at a powder temperature (T_P)=750 °C and T_S=585 °C.[20] Alternatively, when focusing on the early stages of growth, we select a *low growth rate* ($\sim 0.1\ \mu$m/h) regime by reducing T_S and T_P to 575 and 425 °C, respectively.[20] In these conditions, anisotropic growth of CdSe nanostructures was also previously demonstrated.[15]

[a)]Present address: Nokia Research Centre, Cambridge, United Kingdom.
[b)]Electronic mail: acf26@eng.cam.ac.uk.

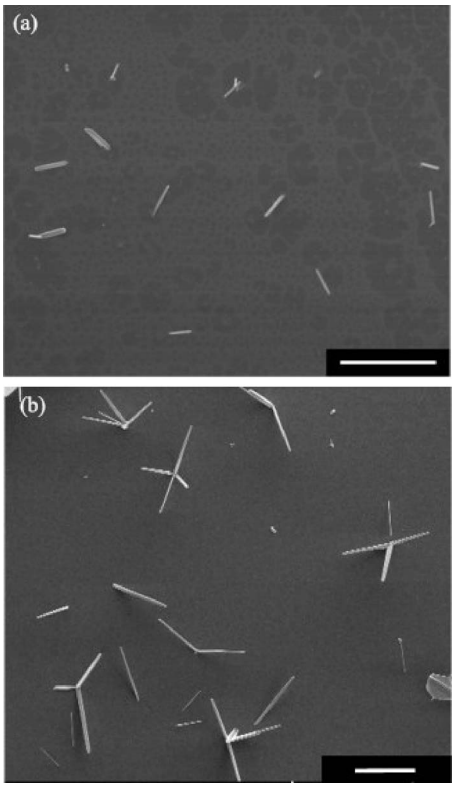

FIG. 1. High-growth-rate synthesis comparison seeded by (a) *s*-NCs and (b) *t*-NCs. When *s*-NCs are used, we observe mainly individual, straight NWs, while for *t*-NCs, we mostly get multibranched nanostructures. Scale bars are 10 μm.

Figures 1(a) and 1(b) show CdSe nanostructures nucleated in the high-growth-rate regime using *s*-NCs and *t*-NCs as seeds The different final morphology is clear. While single, straight NWs are obtained from spherical seeds, *t*-NCs give rise to branched MP structures. After a statistical assessment of the sample surface, we estimate that for sample (a) ~70% of the nanostructures are single and straight NWs, whereas for sample (b) ~75% consists of MPs with two or more branches. We also note that the MP branches in Fig. 1(b) look longer (up to a factor of 2) and slightly thicker than the NWs in Fig. 1(a). Since T_S and T_P (and, thus, the growth rate) are the same in both cases, it is possible that for *s*-NCs a longer incubation time is needed to drive the initial nucleation of a CdSe NW.

Figure 2 shows TEM micrographs of the precursor *s*-NCs distributions [(a) and (c)] and the resulting CdSe nanostructures [(b) and (d)] nucleated in the low-growth-rate regime on SiN membranes. Spin casting of NCs from solution results in both individually dispersed NCs [Fig. 2(a)] and large NC aggregates [Fig. 2(c)]. Figure 2(b) indicates that anysotropic nucleation of a single NW can occur from an individual, spherical seed. When the growth front elongates, the NW diameter gradually expands beyond the initial seed size, indicating that sidewall deposition occurs simultaneously with longitudinal growth, even if with a smaller rate. When *s*-NCs seeds are initially aggregated in a large cluster, though, few NWs are found to nucleate on random locations within the NC agglomerate. Such NWs are usually much thicker than those in Fig. 2(b), and branching [arrow in Fig. 2(d)] occurs more frequently than for individual seeds [Fig. 2(b4)]. Since sidewall deposition proceeds at the same rate in both cases, we conclude that the diameter distribution observed for long NWs grown at high rate [Fig. 1(a)] must depend on the initial NC clustering, with the thinnest NWs stemming from individual seeds. Similarly, the small amount of branched structures statistically reported for the sample in Fig. 1(a) is likely to arise because of seed aggregation and can, thus, be minimized by improving the initial patterning of the *s*-NCs. It must be noted, however, that many individual seeds in Fig. 2(b) do not nucleate any NW. We define "nucleation efficiency" for individual *s*-NCs as the number of nucleated NWs/ number of seeds. This is around 10% for our experiments.

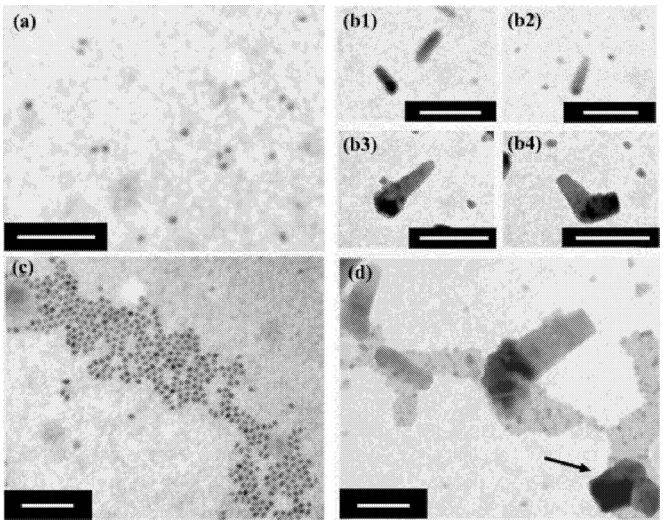

FIG. 2. (a) *s*-NCs individually dispersed on a SiN membrane and (b) corresponding NWs synthesis in low-growth-rate regime. (c) Aggregate *s*-NCs upon dispersion on a SiN membrane and (d) outcome of low-growth-rate synthesis from aggregates. Scale bars are 100 nm.

Figure 3 correlates the original shape and orientation of precursor *t*-NCs [(a), (c), and (e)] with the corresponding CdSe nanostructures after vapor-phase synthesis in the low-growth-rate regime [(b), (d), and (f)]. TEM analysis of the precursor *t*-NCs [(a), (c), and (e)] shows that they usually exhibit a wide distribution of branch number and length, some of the structures being rodlike [Fig. 3(a)]. This may be attributed to a small inhomogeneity during solution-phase synthesis and to fragmentation caused by sonication. Yet, we observe that for most *t*-NCs, vapor-phase anysotropic growth proceeds with further elongation (and thickening) of the original branches, maintaining (even if partially in some cases) the original shape and orientation of the seed. We, thus, believe that the dominant distribution of MPs in Fig. 1(b) is driven by the particular morphology of the individual seeds rather than by agglomeration effects due to seed clustering. The occadional NWs seen in Figs. 1(b) are probably generated by broken tetrapod arms with rodlike morphology, as in Figs. 3(a) and 3(b).

For fixed conditions (low growth rate), the expansion in diameter for the nanostructures in Fig. 3 is more significant, compared to the NWs stemming from individual, spherical seeds (Fig. 2(b)). Also, within the same *t*-NC, some branches appear more efficient than others in promoting CdSe nucleation. The "inefficient" branches may then be incorporated in a larger structure if the neighbor branches continue their growth [Figs. 3(b) and 3(e)]. In other cases some branches seem to completely disappear [Fig. 3(d)]. It is noteworthy, though, that all *t*-NCs give rise to nucleation and elongation from at least one branch. The nucleation efficiency for *t*-NCs

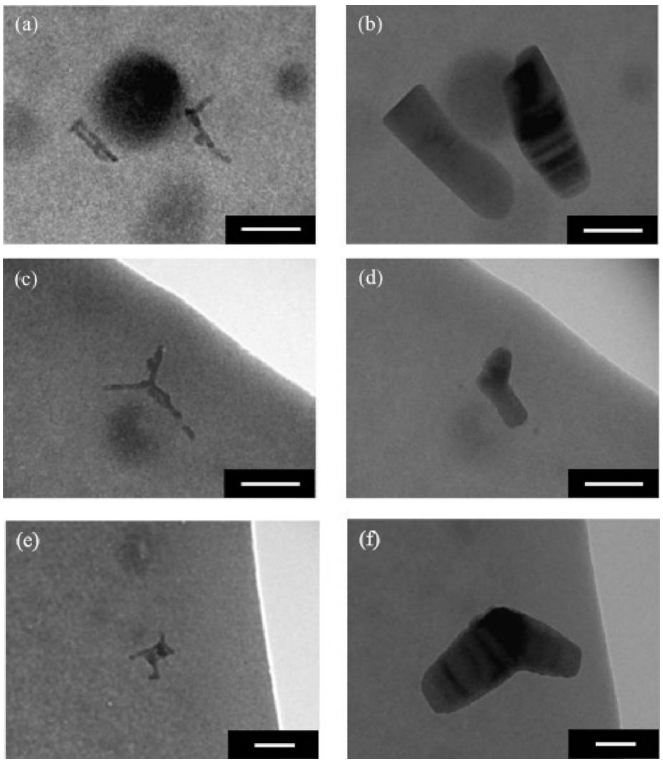

FIG. 3. As-dispersed *t*-NCs (left) and corresponding synthesis of NWs and MPs in low-growth-rate regime (right). Scale bars are 50 nm.

is, therefore, close to 100%, one order of magnitude higher than for individual *s*-NCs.

Most of these effects can be attributed to the extension and nonideal behavior of the NC surfaces. Note that we do not perform any particular treatment of the seeds after their deposition on the substrate to ensure fresh crystalline surfaces for homoepitaxial nucleation. Thus partial oxidation or contamination, due to the presence of surfactants on the NC surfaces, may locally affect the absorption and migration of the impinging CdSe vapor. As a consequence, branches of *t*-NCs can compete for material, which results in some of them failing to grow any further. For spherical seeds, the exposed surface is far smaller than that of *t*-NCs, thus increasing the probability of finding *s*-NCs with inactive surfaces. This may explain the longer (in average) incubation time we observe for NW growth from *s*-NCs (Fig. 1).

Several growth studies, either in solution[23,26] or via vapor-phase,[27,28] indicated that a fine tuning of the reaction kinetics is needed to produce a core seed with the appropriate crystallographic structure. In a single-step process, though, it is difficult to achieve the right compromise between the ideal conditions for seed formation and for the further elongation of the tetrapod arms.[20] Moreover, all nanostructures produced in a single growth run have necessarily the same morphology. Here, we start with already nucleated seeds of well defined geometry, e.g., tetrapods of well-defined crystallographic structure.[26] We then continue the synthesis process by using fixed and optimal conditions for straight NW growth, which, *per-se*, do not introduce any additional branching.[15,20] As an additional benefit, by patterning individual *s*-NCs and *t*-NCs on the same substrate, different nanoshapes can be grown at precise locations during the same growth run.

In summary, we have shown that nanostructure shape selectivity can be achieved by controlling the morphology of the precursor seed. The growth from spherical nanocrystals gives rise preferentially to straight NWs, whereas branching is favored when tetrapod-shaped nanocrystals are used. We also demonstrated that single NWs can originate from individual spherical seeds, and that, for branched NCs, the subsequent growth tends to preserve the original shape and orientation. The suitable patterning of individual NCs may, thus, enable position-selective nanostructure synthesis as accurately as currently achieved through metal nanoparticles.[29]

A. C. F. acknowledges funding from The Royal Society and The Leverhulme Trust. A. F. acknowledges support from Pembroke College, EPSRC, and Cambridge European Trust.

[1]W. U. Huynh, J. J. Dittmer, and A. P. Alivisatos, Science **295**, 2425 (2002).
[2]M. Law, L. E. Greene, J. C. Johnson Richard, and P. Yang, Nat. Mater. **4**, 255 (2005).
[3]X. Duan, Y. Huang, R. H. Agarwal, and C. M. Lieber, Science **421**, 241 (2003).
[4]Y. Huang, X. Duan, and C. M. Lieber, Small **1**, 142 (2005).
[5]Z. R. Dai, Z. W. Pan, and Z. L. Wang, Adv. Funct. Mater. **13**, 9 (2003).
[6]C. Ma, Y. Ding, D. Moore, X. Wang, and Z. L. Wang, J. Am. Chem. Soc. **126**, 708 (2004).
[7]X. T. Zhang, Z. Liu, Y. P. Leung, Quan Li, and S. K. Hark, Appl. Phys. Lett. **83**, 5533 (2003).
[8]L. Manna, E. C. Scher, and A. P. Alivisatos, J. Am. Chem. Soc. **122**, 12700 (2000).
[9]L. Vayssieres, Adv. Mater. (Weinheim, Ger.) **15**, 464 (2003).
[10]L. E. Greene, M. Law, D. H. Tan, M. Montano, J. Goldberger, G. Somorjai, and P. Yang, Nano Lett. **5**, 1231 (2005).
[11]C. H. Liu, J. A. Zapien, Y. Yao, X. Meng, C. S. Lee, S. Fan, Y. Lifschitz, and S. T. Lee, Adv. Mater. (Weinheim, Ger.) **15**, 838 (2003).
[12]L. Zhao, T. Lu, M. Yosef, M. Steinhart, M. Zachrias, U. Gosele, and S. Schelcht, Chem. Mater. **18**, 6094 (2006).
[13]Z. L. Wang, Mater. Today **7**, 26 (2004).
[14]Z. A. Peng and X. G. Peng, J. Am. Chem. Soc. **123**, 183 (2001).
[15]A. Colli, A. Fasoli, S. Hofmann, C. Ducati, J. Robertson, and A. C. Ferrari, Nanotechnology **17**, 1046 (2006).
[16]A. Colli, S. Hofmann, A. C. Ferrari, C. Ducati, F. Martelli, S. Rubini, S. Cabrini, A. Franciosi, and J. Robertson, Appl. Phys. Lett. **86**, 153103 (2005).
[17]P. D. Yang, H. Q. Yan, S. Mao, R. Russo, J. Johnson, R. Saykally, N. Morris, J. Pham, R. He, and H. J. Choi, Adv. Funct. Mater. **12**, 323 (2002).
[18]Z. L. Wang, X. Y. Kong, and J. M. Zuo, Phys. Rev. Lett. **91**, 185502 (2003).
[19]W. I. Park, D. H. Kim, S. W. Jung, and G. C. Yi, Appl. Phys. Lett. **80**, 4232 (2002).
[20]A. Fasoli, A. Colli, S. Kudera, L. Manna, S. Hofmann, C. Ducati, J. Robertson, and A. C. Ferrari, Physica E (Amsterdam) **37**, 138 (2007).
[21]T. Zhai, H. Zhong, Z. Gu, A. Peng, H. Fu, Y. Ma, Y. Li, and J. Yao, J. Phys. Chem. **111**, 2980 (2007).
[22]S. H. Lee, H. J. Lee, D. Oh, S. W. Lee, H. Goto, R. Buckmaster, T. Yasukawa, T. Matsue, S. K. Hong, H. C. Ko, M. W. Cho, and T. Yao, J. Phys. Chem. B **110**, 3856 (2006).
[23]L. Manna, D. J. Milliron, A. Meisel, E. C. Scher, and A. P. Alivisatos, Nat. Mater. **2**, 382 (2003).
[24]J. F. Conley, Jr., L. Stecker, and Y. Ono, Nanotechnology **16**, 292 (2005).
[25]Markers are small holes in the SiN membranes produced by reactive ion-etching.
[26]L. Carbone, S. Kudera, E. Carlino, W. J. Parak, C. Giannini, R. Cingolani, and L. Manna, J. Am. Chem. Soc. **128**, 748 (2006).
[27]H. Iwanaga, M. Fujii, and S. Takeuchi, J. Cryst. Growth **134**, 275 (1993).
[28]C. Ronning, N. G. Shang, I. Gerhards, H. Hofsäss, and M. Seibt, J. Appl. Phys. **98**, 034307 (2005).
[29]T. Martensson, P. Carlberg, M. Borgstrom, L. Montelius, W. Seifert, and L. Samuelson, Nano Lett. **4**, 699 (2004).